Research Article | Vol. 25, No. 3 | 6 Feb 2017 | OPTICS EXPRESS 2618

Optics EXPRESS

Wavelength tuning of the spirally drawn whispering gallery mode microfiber lasers and the perspectives for sensing applications

SHANCHENG YANG,[1] TAY YONG KANG EUGENE,[1] YUE WANG,[1] XIN ZHAO,[1] HILMI VOLKAN DEMIR,[1,2,3,4] AND HANDONG SUN[1,4,*]

[1]*Division of Physics and Applied Physics, School of Physical and Mathematical Sciences, Nanyang Technological University, Singapore 637371, Singapore*
[2]*School of Electrical and Electronic Engineering, LUMINOUS! Center of Excellence for Semiconductor Lighting and Displays, Nanyang Technological University, Nanyang Avenue, Singapore 639798, Singapore*
[3]*Department of Electrical and Electronics Engineering and Department of Physics, UNAM – Institute of Materials Science and Nanotechnology, Bilkent University, Bilkent, Ankara TR-06800, Turkey*
[4]*Centre for Disruptive Photonic Technologies (CDPT), School of Physical and Mathematical Sciences, Nanyang Technological University, Singapore 637371, Singapore*
[*]*hdsun@ntu.edu.sg*

Abstract: Facile and cost-efficient microcavities, as well as the tuning of the optical modes, especially for the application of top-grade optical devices, have been emerging as attractive research fields. In this work, controllable fabrication of the microfiber laser arrays in polymer matrix is achieved by employing the advanced spiral drawing technique. Besides the high-quality whispering gallery mode (WGM) lasing, wavelength tuning is also realized by applying external forces on the polymer matrix, which induce slightly enlarged cavity sizes. Furthermore, the perspectives of utilizing the microfiber arrays as force and strain sensors are discussed and demonstrated.

OCIS codes: (060.2370) Fiber optics sensors; (060.3510) Lasers, fiber; (140.3410) Laser resonators; (140.3945) Microcavities; (140.3948) Microcavity devices.

References and links

1. K. J. Vahala, "Optical microcavities," Nature **424**(6950), 839–846 (2003).
2. V. S. Ilchenko and A. B. Matsko, "Optical resonators with whispering-gallery modes-part II: applications," IEEE J. Sel. Top. Quantum Electron. **12**(1), 15–32 (2006).
3. Y. Wang, V. D. Ta, Y. Gao, T. C. He, R. Chen, E. Mutlugun, H. V. Demir, and H. D. Sun, "Stimulated emission and lasing from CdSe/CdS/ZnS core-multi-shell quantum dots by simultaneous three-photon absorption," Adv. Mater. **26**(18), 2954–2961 (2014).
4. Y. Wang, S. Yang, H. Yang, and H. D. Sun, "Quaternary alloy quantum dots: toward low-threshold stimulated emission and all-solution-processed lasers in the green region," Adv. Opt. Mater. **3**(5), 652–657 (2015).
5. G. Righini, Y. Dumeige, P. Féron, M. Ferrari, G. Nunzi Conti, D. Ristic, and S. Soria, "Whispering gallery mode microresonators: fundamentals and applications," Riv. Nuovo Cim. **34**(7), 435–488 (2011).
6. S. Yang, Y. Wang, and H. D. Sun, "Advances and prospects for whispering gallery mode microcavities," Adv. Opt. Mater. **3**(9), 1136–1162 (2015).
7. V. D. Ta, R. Chen, and H. D. Sun, "Self-assembled flexible microlasers," Adv. Mater. **24**(10), OP60–OP64 (2012).
8. L. He, Ş. K. Özdemir, and L. Yang, "Whispering gallery microcavity lasers," Laser Photonics Rev. **7**(1), 60–82 (2013).
9. Y. Wang, K. E. Fong, S. Yang, V. D. Ta, Y. Gao, Z. Wang, V. Nalla, H. V. Demir, and H. D. Sun, "Unraveling the ultralow threshold stimulated emission from CdZnS/ZnS quantum dot and enabling high-Q microlasers," Laser Photonics Rev. **9**(5), 507–516 (2015).
10. F. Monifi, J. Friedlein, Ş. K. Özdemir, and L. Yang, "A robust and tunable add-drop filter using whispering gallery mode microtoroid resonator," J. Lightwave Technol. **30**(21), 3306–3315 (2012).
11. D. O'Shea, C. Junge, J. Volz, and A. Rauschenbeutel, "Fiber-optical switch controlled by a single atom," Phys. Rev. Lett. **111**(19), 193601 (2013).

#281506 https://doi.org/10.1364/OE.25.002618
Journal © 2017 Received 30 Nov 2016; revised 26 Jan 2017; accepted 27 Jan 2017; published 1 Feb 2017

Optics EXPRESS

12. L. Liu, R. Kumar, K. Huybrechts, T. Spuesens, G. Roelkens, E. J. Geluk, T. de Vries, P. Regreny, D. Van Thourhout, and R. Baets, "An ultra-small, low-power, all-optical flip-flop memory on a silicon chip," Nat. Photonics **4**(3), 182–187 (2010).
13. V. D. Ta, R. Chen, D. M. Nguyen, and H. D. Sun, "Application of self-assembled hemispherical microlasers as gas sensors," Appl. Phys. Lett. **102**(3), 031107 (2013).
14. L. Chang, X. Jiang, S. Hua, C. Yang, J. Wen, L. Jiang, G. Li, G. Wang, and M. Xiao, "Parity-time symmetry and variable optical isolation in active-passive-coupled microresonators," Nat. Photonics **8**(7), 524–529 (2014).
15. V. D. Ta, R. Chen, and H. D. Sun, "Tuning whispering gallery mode lasing from self-assembled polymer droplets," Sci. Rep. **3**, 1362 (2013).
16. V. D. Ta, R. Chen, and H. D. Sun, "Coupled polymer microfiber lasers for single mode operation and enhanced refractive index sensing," Adv. Opt. Mater. **2**(3), 220–225 (2014).
17. R. Chen, V. D. Ta, and H. D. Sun, "Bending-induced bidirectional tuning of whispering gallery mode lasing from flexible polymer fibers," ACS Photonics **1**(1), 11–16 (2014).
18. S. Yang, V. D. Ta, Y. Wang, Y. Gao, T. He, R. Chen, H. V. Demir, and H. D. Sun, "Multicolor lasing prints," Appl. Phys. Lett. **107**(22), 221103 (2015).
19. S. Yang, V. D. Ta, Y. Wang, R. Chen, T. He, H. V. Demir, and H. Sun, "Reconfigurable Liquid Whispering Gallery Mode Microlasers," Sci. Rep. **6**, 27200 (2016).
20. S. K. Tang, R. Derda, Q. Quan, M. Lončar, and G. M. Whitesides, "Continuously tunable microdroplet-laser in a microfluidic channel," Opt. Express **19**(3), 2204–2215 (2011).
21. C. L. Linslal, M. Kailasnath, S. Mathew, T. K. Nideep, P. Radhakrishnan, V. P. Nampoori, and C. P. Vallabhan, "Tuning whispering gallery lasing modes from polymer fibers under tensile strain," Opt. Lett. **41**(3), 551–554 (2016).
22. R. Madugani, Y. Yang, J. M. Ward, J. D. Riordan, S. Coppola, V. Vespini, S. Grilli, A. Finizio, P. Ferraro, and S. Nic Chormaic, "Terahertz tuning of whispering gallery modes in a PDMS stand-alone, stretchable microsphere," Opt. Lett. **37**(22), 4762–4764 (2012).
23. Z. Zhou, F. Shu, Z. Shen, C. Dong, and G. C. Guo, "High-Q whispering gallery modes in a polymer microresonator with broad strain tuning," Sci. China Phys. Mech. Astron. **58**(11), 114208 (2015).
24. M. Humar, M. Ravnik, S. Pajk, and I. Muševič, "Electrically tunable liquid crystal optical microresonators," Nat. Photonics **3**(10), 595–600 (2009).
25. A. Kiraz, A. Kurt, M. Dündar, and A. Demirel, "Simple largely tunable optical microcavity," Appl. Phys. Lett. **89**(8), 081118 (2006).
26. T. Ioppolo, U. Ayaz, and M. V. Otügen, "Tuning of whispering gallery modes of spherical resonators using an external electric field," Opt. Express **17**(19), 16465–16479 (2009).
27. V. D. Ta, R. Chen, L. Ma, Y. J. Ying, and H. D. Sun, "Whispering gallery mode microlasers and refractive index sensing based on single polymer fiber," Laser Photonics Rev. **7**(1), 133–139 (2013).
28. F. Sajed and C. Rutherglen, "All-printed and transparent single walled carbon nanotube thin film transistor devices," Appl. Phys. Lett. **103**(14), 143303 (2013).
29. M. Saito, H. Shimatani, and H. Naruhashi, "Tunable whispering gallery mode emission from a microdroplet in elastomer," Opt. Express **16**(16), 11915–11919 (2008).
30. C. Lam, P. T. Leung, and K. Young, "Explicit asymptotic formulas for the positions, widths, and strengths of resonances in Mie scattering," J. Opt. Soc. Am. B **9**(9), 1585–1592 (1992).
31. R. Chen and H. D. Sun, "Single mode lasing from hybrid hemispherical microresonators," Sci. Rep. **2**, 244 (2012).
32. T. Ioppolo, M. Kozhevnikov, V. Stepaniuk, M. V. Otügen, and V. Sheverev, "Micro-optical force sensor concept based on whispering gallery mode resonators," Appl. Opt. **47**(16), 3009–3014 (2008).
33. M. G. Allen, M. Mehregany, R. T. Howe, and S. D. Senturia, "Microfabricated structures for the insitu measurement of residual stress, young's modulus, and ultimate strain of thin films," Appl. Phys. Lett. **51**(4), 241–243 (1987).
34. J. Albert, L. Y. Shao, and C. Caucheteur, "Tilted fiber Bragg grating sensors," Laser Photonics Rev. **7**(1), 83–108 (2013).
35. M. Manzo, T. Ioppolo, U. K. Ayaz, V. Lapenna, and M. V. Ötügen, "A photonic wall pressure sensor for fluid mechanics applications," Rev. Sci. Instrum. **83**(10), 105003 (2012).

1. Introduction

Optical microcavities have aroused enormous research interests in the past decades due to the abundant applications in lasers, optoelectronics, chaos studies and quantum electrodynamics [1–4]. Among all of the cavity geometries, the whispering gallery mode (WGM) configuration, formed by trapping light inside the cavity via total internal reflections, are advantageous for their high quality (Q) factor, small mode volume and large optical density, which induce enhanced light-matter interaction [5, 6]. Meanwhile, high-Q lasers can also be achieved by embedding active materials into the microcavities [7–9] and various practical applications have been developed with WGM microcavities and microlasers, including add-

Optics EXPRESS

drop filters, switches, memories, optical isolator, biological and chemical sensors, etc [10–14].

The majority of the conventional microcavities can only provide stationary resonances limited by the solid nature of the cavity materials [6], which hinders their potential in a variety of applications. In contrast, soft-approached materials, represented by polymers, are attractive not only because of their intrinsic flexibility and optical transparency properties, but also the simple processing and low cost [6]. Instead of sophisticated processing procedures, the reported polymer microspheres, hemispheres, floating quasi-disk microlasers, microfibers are self-assembled and fabricated by straightforward techniques, such as tip-touching, direct drawing, inject printing, etc [15–19]. These flexible WGM microcavities and microlasers with facile tunability compensate the deficiency of the solid ones and, thus, further broaden the practical applications in optical devices.

In general, the resonances of the WGM microcavities are ultrasensitive to the gain material, the effective index and the cavity geometry [6]. As the modification of the gain medium is relatively difficult after fabrication, most of the wavelength-tuning works for soft-approached WGM microlasers are based on the manipulation of the cavity size or the variation of the effective index [17, 19–23]. However, the proposed works require complex setups such as a fluidic channel, external electromagnetic fields, or an environmental-controllable chamber to tune the lasing peaks, which are inconvenient for practical applications [20, 24–26]. On the other hand, the polymer fibers, when doped with active gain medium, are unique as they hold the potential to serve as laser sources and waveguides simultaneously [27]. Meanwhile, the superb optical performances of the microfiber lasers when buried inside a protection matrix [17], together with the intrinsic elasticity of the polymer materials, ensure the microfibers to be promising candidates for facile and simple wavelength tuning induced by cavity deformation. However, the reported manual direct drawing technique of the polymer microfibers lacks control of both the diameter and position, which results in a coarse resolution and obstructs the development of this competitive configuration.

In this work, we propose and demonstrate a controllable fabrication technique of the dye-doped polymer microfiber arrays by spiral drawing method. The microfiber arrays were buried in the polydimethylsiloxane (PDMS) matrix for protection and the position could be manipulated by a microplotter with the resolution of 1μm. High-quality WGM lasing was achieved and tuned by utilizing the elastic property of the PDMS matrix as well as the microfiber materials. Quantitative studies reveal that the system can be utilized as a novel approach to sense the strain or force perturbations with the sensitivity of 0.45 pm/με and 5.66 nm N^{-1}, respectively. Our work not only provides a manageable technique for polymer microfiber array fabrication, but also gives the prospect to a highly reliable sensing system which has the potential to be applied in multi-point ultra-small vibration detection and structural health monitoring.

2. Spiral drawing of the microfiber lasers

The host materials for the microfiber lasers were epoxy resin and polymethylmethacrylate (PMMA). The epoxy resin is chosen due to its transparent, stable and viscous properties [7] while the PMMA plays the role of viscosity modulation in the mixed solution [27]. Rhodamine B (RhB, 20 mg), acting as the active material in the microfiber laser, was dissolved in dichloromethane (CH_2Cl_2, 5 mL, 6.4g, purity 99.76%) and then the PMMA powder and the epoxy resin were added into the solution in sequence with the mass ratio of $m_{CH_2Cl_2} : m_{PMMA} : m_{epoxy} = 64 : 3 : 7.5$, $m_{PMMA} : m_{epoxy} = 0.4$. Finally, half hour of ultrasonic vibration was exploited to the mixture, which resulted in the transparent and homogeneous host solution for the microfiber lasers.

The GIX Microplotter II from Sonoplot, INC was employed for the fabrication of the microfibers. With micrometer-level flexible control of the motors and abundant fabrication

Optics EXPRESS

techniques like inkjet printing, plotting and drawing, the microplotter has been proved to be a powerful tool in micro-structure design and implementation, especially for the soft materials [19, 28, 29]. As shown in Fig. 1(a), the host solution was absorbed into the hollow glass dispenser due to the capillary effect when the tip touched the solution droplet. Then the dispenser was lifted up for a certain height of *h* as shown in Fig. 1(b). Due to the viscosity and the surface tension of the solution, a straight cylindrical line was formed between the tip of the dispenser and the solution droplet, which formed the precursor of the microfiber array. A rotational motor with the sample substrate fixed at the center was operated in close proximity to the precursor with the help of the X-Y-Z stage, which is illustrated in Fig. 1(c). The glass sample substrate (30 mm × 30 mm × 1 mm) was previously covered with uncured PDMS elastomer (Sylgard 184 from Dow Corning), which is not only optically and chemically inert, but also provides low refractive index and good mechanical flexibility [17]. The sample substrate served as a spool in the fabrication process and after the motor rotating spirally, the microfiber array was fabricated and buried in the PDMS matrix with constant spacing and uniform diameters as shown in Fig. 1(d). Finally, the sample substrate was heated in the oven at 50℃ for three hours to fully cure the PDMS matrix. After cutting the edge of the substrate to separate the fibers buried in the polymer matrix and the ones stuck on the back of the glass, the solidified elastic PDMS matrix, together with the microfiber array buried inside, could be separated from the glass substrate manually.

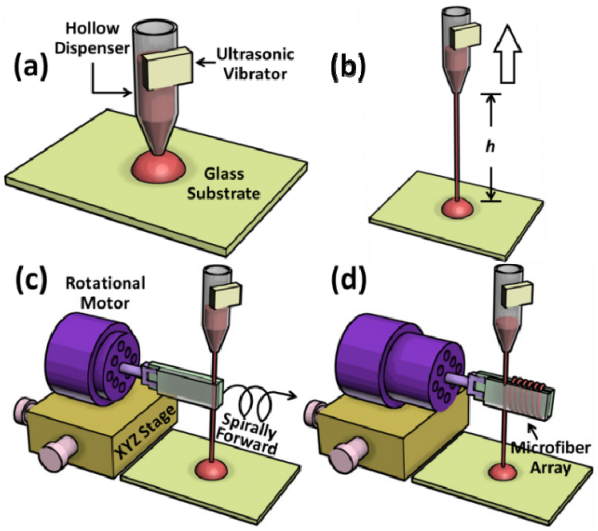

Fig. 1. (a) Absorption of the fiber solution due to the capillary effect. (b) Formation of the microfiber precursor by lifting up the dispenser of the microplotter with a certain height. (c) Approaching of the spirally rotating motor with uncured on-substrate PDMS matrix at the center. (d) Fabricated microfiber array buried in the PDMS matrix.

The position of the microfibers could be controlled by the X-Y-Z stage as well as the rotating and advancing speed ratio of the motor as shown in Figs. 2(a) and 2(b). Meanwhile, the diameter of the microfibers in a set of array was the same as the diameter of the cylindrical microfiber precursor, which was inversely proportional to the lift-up height of the dispenser as plotted in Fig. 2(c). As the solutions in the droplet and the dispenser both provided sufficient materials during the rolling process, the diameter of the precursor was expected to be constant and therefore, the microfibers in the PDMS matrix presented uniform size. The standard deviations for the samples measured in each lifting height are around 0.24 μm. Figure 2(d) illustrates the reproducibility of the spirally drawing technique. With the lifting height fixed at 10 cm, the average microfiber diameters for the three independent sets (five microfibers in each set) are 16.073 μm, 16.396 μm and 16.402 μm, respectively. It is

Optics EXPRESS

important to note that the all the microfibers are measured three times from the top, middle and bottom of the optical images to ensure the uniformity of the cylindrical samples.

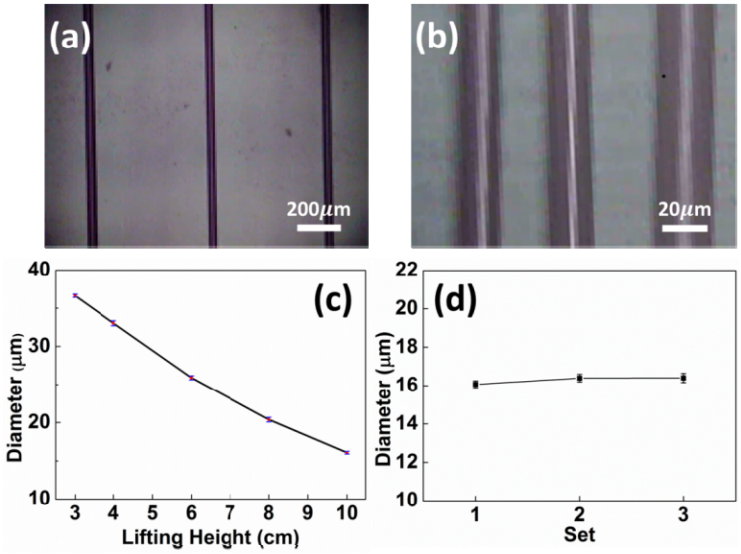

Fig. 2. (a)-(b) Optical images of the fabricated microfiber arrays with different periods and diameters. (c) The dependence of microfiber diameter on the lifting height of the dispenser. (d) The reproducibility test of the spirally drawing technique. The lifting heights of the dispenser for the three independent sets are all 10 cm.

3. Characterization of the WGM lasing

A micro-photoluminescence (μ-PL) system was setup to investigate the optical performances of the microfiber lasers. The microfibers, along with the PDMS matrix, were placed on a controllable X-Y-Z platform. The excitation source was chosen to be a 532 nm Q-switched Nd: YAG laser with the repetition rate of 60 Hz, pulse width of 1 ns and incident angles of 45° and 90° with respect to the X-Y-Z platform and the microfibers, respectively. The excitation beam spot was adjusted to cover only one microfiber in the matrix. Then the emitted signal from the single microfiber laser was collected by a 50X objective (numerical aperture = 0.42, set above the polymer matrix, see Fig. 3(a)) and recorded by a silicon charge-coupled device (CCD) through a low-loss commercial optical fiber.

Although several microfibers were burried in the same PDMS matrix, only one was measured for optical characterization due to the consistency of the microfibers and the recorded photoluminescence (PL) spectrum of the microfiber lasers is shown in Fig. 3(b). Lasing can be clearly observed from the appearance of the sharp peaks in spectrum. It is known that the WGM resonances are determined by numerous factors including the cavity radius R, refractive indices of the microcavity (n_{cav}) and the surrounding (n_{env}), longitudinal mode number m, radial mode number r, and azimuthal peak number $l - m + 1$ [19, 20, 30]. Due to the relatively high Q factors, the fundamental modes are much easier to be observed in experiments than the higher order modes [6]. Thus, the characterization equation can be simplified to:

$$\lambda_{\mathrm{TM}} \approx \frac{2\pi R n_{cav}}{m + 1.856 m^{\frac{1}{3}} + \left(\frac{1}{2} - \frac{n_{env}^2}{n_{cav}\sqrt{n_{cav}^2 - n_{env}^2}}\right)}. \quad (1)$$

With the cavity and PDMS matrix refractive indices of 1.47 and 1.41 [17], respectively, the calculated fundamental TM modes match closely with the experimental results (Fig. 3(b)).

Optics EXPRESS

In addition, the Q factor, which is experimentally defined as the resonant wavelength (λ) over the full width half maximum (FWHM), is in the order of 10^3 and proportional to the diameter of the microfiber. Thus, together with the bright edges of the excited microfiber shown in the inset of Fig. 3(b), the mechanism is confirmed to be WGM lasing. Detailed investigation of the power-dependent experiment, which indicates the evolution from broadband emission to lasing and the lasing threshold, can be found in our previously reported work with the similar geometry [17]. In addition, single mode lasing was also observed in the microfiber laser with small diameter (Fig. 3(c)) because of the relatively high cavity loss for other resonant modes [31].

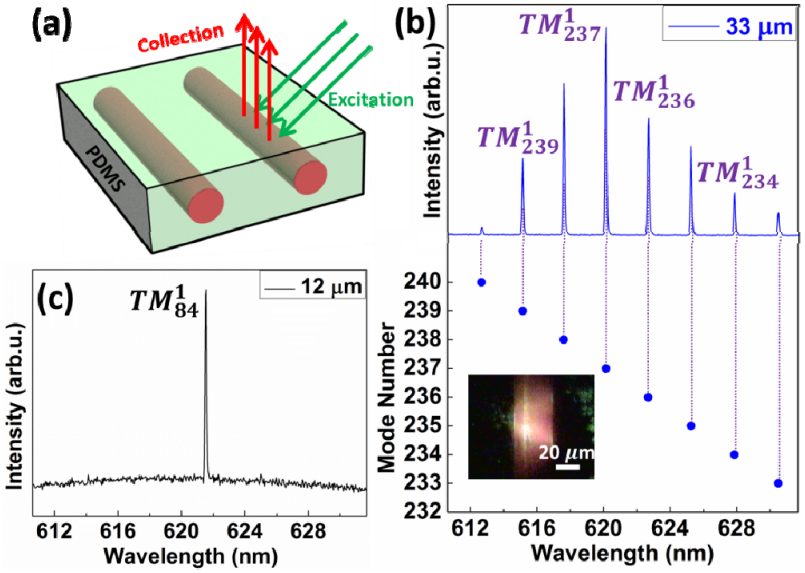

Fig. 3. (a) Schematic of the excitation and collection system. (b) Spectrum of the microfiber under excitation and mode allocation. Inset shows the microfiber laser under excitation. (c) Single mode lasing in the excited 12-μm microfiber.

4. Deformation-induced wavelength tuning and the sensing applications

As the PDMS matrix permits mechanical extension due to the intrinsic elastic properties, it is possible to tune the lasing peaks via the external-force-induced deformation of the microfiber lasers. As shown in Fig. 4(a), the PDMS matrix with the 33 μm-microfiber buried inside was fixed on a stationary matrix holder at one end while leaving the other end moveable. Figure 4(b) illustrates that with the extension of the PDMS matrix, the lasing modes show regular redshift. This phenomenon can be explained by the cavity-size enlargement model. By stretching the PDMS matrix, the circular cross-section of the microfiber was deformed to ellipse, which induced a larger WGM perimeter [15]. Thus, the new resonant condition is:

$$(n_{eff} + \Delta n_{eff})[\pi\sqrt{2(a^2 + b^2)}] = m(\lambda + \Delta\lambda). \tag{2}$$

where n_{eff} is the effective index, a and b are the half length of the major and minor axis of the ellipsoid cross-section, respectively. Equation (2) can be transformed to:

$$\frac{\Delta\lambda}{\lambda} = \sqrt{\frac{a^2 + b^2}{2R^2}} - 1 + \sqrt{\frac{a^2 + b^2}{2R^2}}\frac{\Delta n}{n}. \tag{3}$$

Optics EXPRESS

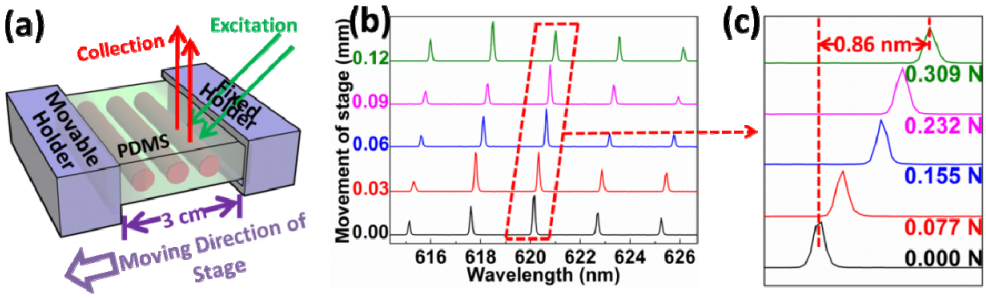

Fig. 4. (a) Schematic of the force applying system. (b) Spectrum of the lasing modes with respect to the stage movement. Redshifting can be seen clearly with the lengthening of the matrix. (c) Enlarged spectrum in (b) with calculated forces and mode shift range.

Equation (3) illustrates that the wavelength shift is due to the change of both the cavity circumference and the effective index. However, the two factors compete with each other as the enlargement of the cavity size promotes redshift of the spectrum while the "dilution" of the material under tension decreases the effective index, which results in the blueshift of the lasing peaks [15, 17]. The experimental results shown in Fig. 4(b) indicate that the dominant factor in this work is the change of the cavity size. Therefore, Eq. (3) can be further simplified with the negligence of the effective index:

$$\frac{\Delta\lambda}{\lambda} = \sqrt{\frac{a^2 + b^2}{2R^2}} - 1. \tag{4}$$

With 0.12 mm elongation of the PDMS matrix, the a and b of the ellipsoid cross-section is calculated to be 16.57 μm and 16.48 μm, respectively (The values of a and b are obtained from the assumption that under uniform elongation, the percentage of changing is the same for the matrix and the fiber radius). Substituting the parameters into Eq. (4) yields $\Delta\lambda$ = 0.85 nm, which is consistent with experimental measurement in Fig. 4(c).

The tuning of the lasing peaks can be implemented in force and strain sensing. In comparison with the rigid glassy and semiconductor materials, our soft PDMS-fiber system is expected to possess higher sensitivity for tiny force or pressure vibrations [32], which can be further applied in ultra-precision instrument calibration and maintenance. The forces applied on the PDMS elastic matrix can be calculated via the linear Young's modulus model [33] (The Young's modulus of PDMS under ambient conditions is obtained from the database of Sandia National Laboratories) and the calculated maximum force applied in Fig. 4(c) was 0.309 N, which resulted in a force sensitivity of 2.78 nm·N^{-1} and a strain sensitivity of 0.22 pm/με.

To further improve the strain and force sensitivity, we conducted size dependent and composition ratio dependent experiments. The composition ratio refers to the polymethylmethacrylate (PMMA) to epoxy resin mass ratio in the host solution of the microfibers. As shown in the blue curve in Fig. 5, the sensitivity is proportional to the diameter of the microfibers at consistent PMMA to epoxy resin mass ratio. This is because the circumference change for the large-diameter microfibers is greater than the small ones under the same fraction of elongation. As the PMMA is used as the viscosity modulator in the microfiber solution, large PMMA to epoxy resin mass ratio will induce the high viscosity or rigidity of the microfiber, which makes the cross-section difficult to be deformed. Hence, sensitivity droop can be observed with the increase of the PMMA to epoxy resin mass ratio (red curve in Fig. 5). The highest sensitivity for the microfiber laser was measured to be 0.45 pm/με (strain) and 5.66 nm·N^{-1} (force) with the fiber diameter of 45 μm and PMMA to epoxy resin mass ratio of 0.4, which is similar to the previously reported spherical WGM sensors [29, 32]. As the minimum distinguishable mode shift of the microfiber laser is determined by the FWHM [19], the limit of detection of the 45-μm microfiber laser is calculated to be 1.76 ×

Optics EXPRESS

10^{-4} ε (strain) and 0.014 N (force). It is important to note that the PMMA to epoxy resin mass ratio cannot be further decreased because 0.4 is the minimum value to maintain the shape of a fiber. Otherwise the microfibers will breakdown into microspheres due to the huge surface tension of the solution [13]. Although the sensing performances are not as good as the widely applied fiber Bragg grating (FBG) sensors and the passive PDMS microdroplets [22, 23, 34], the novel approached microfiber sensors have huge space for improvement. Indeed, except for the sensitivity, the microfiber array structure is more manageable and practical than the reported self-assembled microbottle-force-sensors that are exposed to air contaminants [22, 23]. Further studies for increasing the force sensitivity by minimizing the width of the PDMS matrix, improving the *Q* factors with more advanced fabrication technique, selecting other elastic materials with lower refractive indices for the protection matrix, and simplifying the excitation/collection system all advance the WGM strain sensors to be more competitive.

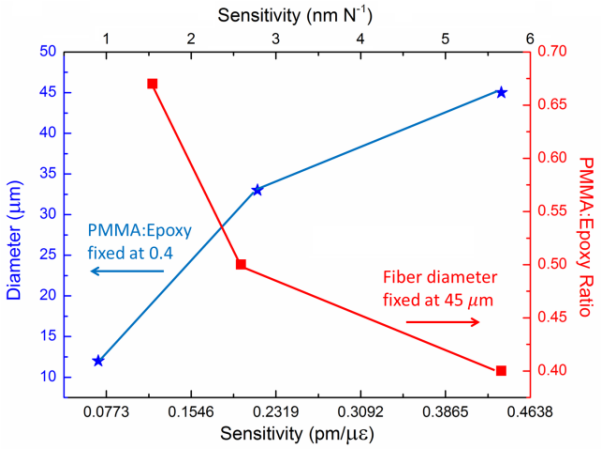

Fig. 5. The PMMA: Epoxy mass ratio and diameter dependence on the sensor sensitivities of strain and force.

One of the major concerns of the dye-doped microlaser is the thermal-induced shift caused by long-time excitation [27], which decreases the reliability of the sensing applications. However, our design can avoid this feint shifting by alternating or scanning the microfibers with high homogeneity in the array, which improves the sensing reliability. In addition, comparing with conventional WGM strain sensors which are exposed and may show different sensitivities in various working environments [32, 35], our microfiber lasers are supposed to perform stably with constant sensitivity due to the PDMS matrix, which provides consistent environmental refractive index to stabilize the lasing peaks. Besides, the reported wavelength tuning of microfibers based on axial strain or refractive index modification [17, 21], together with the theoretically unlimited WGM planes (cross-sections) of the cylindrical geometry, enables the microfiber configuration to be utilized as multi-directional and multi-point sensors, which is more convenient and multifunctional than the single-element-based geometries [17].

5. Conclusions

In conclusion, we have fabricated microfiber laser arrays buried in PDMS matrix by the spiral drawing technique. The diameters and the position of the microfibers could be controlled by adjusting appropriate parameters. High-quality WGM lasing was observed and investigated. Meanwhile, redshift of the lasing modes under stretching forces of the PDMS matrix was achieved and proposed as strain and force sensors with the sensitivity of 0.45 pm/ με and 5.66 nm N^{-1}, respectively. Our work not only reveals a simple and robust setup for wavelength tuning, but also demonstrates a novel approach for strain and force sensing. The potential to

Optics EXPRESS

realize multi-point and multi-directional sensing, as well as the enhanced reliability provided by the array structure and PDMS matrix enable the device to be promising in practical applications.

Funding

Singapore National Research Foundation (No. NRFCRP6-2010-02); Singapore Ministry of Education (Projects MOE 2011-T3-1-005 and Tier 1- RG92/15).

Acknowledgment

We thank all the authors for their insightful discussions.